

Article

## Synthesis, Thermal Stability and Properties of ZnO Nanoparticles

W. Chen, Y. H. Lu, M. Wang, L. Kroner, H. Paul, H.-J. Fecht, J. Bednarcik, K. Stahl, Z. L. Zhang, U. Wiedwald, U. Kaiser, P. Ziemann, T. Kikegawa, C. D. Wu, and J. Z. Jiang

*J. Phys. Chem. C*, **2009**, 113 (4), 1320-1324 • DOI: 10.1021/jp808714v • Publication Date (Web): 05 January 2009

Downloaded from <http://pubs.acs.org> on February 10, 2009

### More About This Article

Additional resources and features associated with this article are available within the HTML version:

- Supporting Information
- Access to high resolution figures
- Links to articles and content related to this article
- Copyright permission to reproduce figures and/or text from this article

[View the Full Text HTML](#)



ACS Publications  
High quality. High impact.

Synthesis, Thermal Stability and Properties of ZnO<sub>2</sub> Nanoparticles

W. Chen,<sup>†</sup> Y. H. Lu,<sup>†</sup> M. Wang,<sup>‡</sup> L. Kroner,<sup>§</sup> H. Paul, H.-J. Fecht,<sup>§</sup> J. Bednarcik,<sup>||</sup> K. Stahl,<sup>⊥</sup> Z. L. Zhang,<sup>#</sup> U. Wiedwald,<sup>∇</sup> U. Kaiser,<sup>#</sup> P. Ziemann,<sup>∇</sup> T. Kikegawa,<sup>○</sup> C. D. Wu,<sup>‡</sup> and J. Z. Jiang<sup>\*,†</sup>

International Center for New-Structured Materials (ICNSM), and Laboratory of New-Structured Materials, Department of Materials Science and Engineering, Zhejiang University, Hangzhou 310027, P. R. China, Department of Chemistry, Zhejiang University, Hangzhou 310027, P. R. China, Department of Materials, Faculty of Engineering, University of Ulm, Albert-Einstein Allee 47, D-89081 Ulm, Germany, HASYLAB am DESY, Notkestrasse 85, D-22603 Hamburg, Germany, Department of Chemistry, Technical University of Denmark, DK-2800 Lyngby, Denmark, Electron Microscopy Group of Materials Science, University of Ulm, D-89069 Ulm, Germany, Department of Solid State Physics, University of Ulm, Albert-Einstein Allee 11, D-89081 Ulm, Germany, and Photon Factory, Institute for Materials Structure Science, High Energy Accelerator Organization, 1-1, Oho, Tsukuba 305-0801, Japan

Received: October 2, 2008; Revised Manuscript Received: November 6, 2008

ZnO<sub>2</sub> nanoparticles have been synthesized by an organometallic precursor method. The structure, structural stability, and magnetic and optical properties of ZnO<sub>2</sub> nanoparticles have been investigated by experiments and first-principles calculations. It is found that ZnO<sub>2</sub> nanoparticles decompose into ZnO at about 230 °C and is stable up to 36 GPa at ambient temperature. The cubic ZnO<sub>2</sub> phase has a bulk modulus of  $B_0 = 174$  GPa at zero pressure. Nanocrystalline ZnO<sub>2</sub> material is an indirect semiconductor with an energy gap of about 4.5 eV and paramagnetic down to 5 K.

## Introduction

Nanocrystals, consisting of small crystallites of diameter 1–500 nm, often have novel physical and chemical properties differing from those of the corresponding bulk materials.<sup>1,2</sup> For example, nanometer-sized semiconductors have electronic and optical properties that depend on the particle size, making them potential candidates for applications where tunability of these properties is essential. The unique properties of nanocrystalline materials open up the general question of how crystallite size and shape affect the structural stability.

Zinc peroxide (ZnO<sub>2</sub>) is mostly used in the rubber industry<sup>3–5</sup> and plastic processing.<sup>6,7</sup> It can also be used as an oxidant for explosives and pyrotechnic mixtures.<sup>8</sup> Nanoparticles of zinc peroxide can additionally be used as precursors for preparation of ZnO nanoparticles.<sup>9,10</sup> Here we report results for ZnO<sub>2</sub> nanoparticles, prepared by a chemical method. Structural stability of ZnO<sub>2</sub> nanoparticles were studied at temperatures up to 800 °C and pressures up to 36 GPa together with optical and magnetic properties measurements and first-principles calculations.

## Experimental Section

**Synthesis.** Nanometer-sized ZnO<sub>2</sub> nanoparticles were synthesized by an organometallic precursor method. ZnCl<sub>2</sub> (0.136 g) was dissolved in 22.46 mL of THF under vacuum at room temperature for 30 min. Then, Mg(C<sub>6</sub>H<sub>11</sub>)Cl (1.54 mL 1.3 M

solution in THF) and 1-octylamine (OA, 99%) were slowly injected into the ZnCl<sub>2</sub> solution, which was heated to 323 K for 48 h. H<sub>2</sub>O<sub>2</sub> (30 mL) was then added to disperse the precipitate. The dispersed solution was semitransparent after 6 h. The precipitate in the solution was separated by centrifugation and washed several times with distilled water and alcohol. The precipitate was dried into powder in air.

**Characterization.** The structure and average crystallite size of ZnO<sub>2</sub> nanoparticles were determined by X-ray diffraction (XRD) using a Co K<sub>α</sub> radiation and Rietveld refinement. The Rietveld refinement program is a local variation of the LHMP1 program,<sup>11</sup> using the pseudo-Voigt profile function and Chebyshev polynomial background fitting. High resolution transmission electron microscopy measurements for the sample, prepared by dropping the liquid containing ZnO<sub>2</sub> nanoparticles on a carbon-coated copper grid, were performed using Titan FEI 80-300 equipped with a field emission gun. The composition ratio of Zn:O was examined by electron energy-loss spectroscopy (EELS).

To evaluate the structural stability of ZnO<sub>2</sub> nanoparticles, temperatures up to 800 °C or pressures up to 36 GPa for in situ XRD measurements were performed together with thermogravimetry (TG) measurements up to 400 °C in air. In situ high temperature XRD measurements for ZnO<sub>2</sub> nanoparticles in a quartz capillary in air were carried out at beamline B2 ( $\lambda = 0.49334(5)$  Å) at HASYLAB/DESY, Hamburg. The sample was annealed with a step of 10 °C in the temperature range of 50–250 °C and of 50 °C in the temperature range of 250–800 °C and was exposed to an X-ray beam for about 20 min. For in situ high pressure XRD measurements at ambient temperature, a powder sample was placed into the diamond anvil cell (DAC) using diamonds with 360  $\mu$ m diameter culets. The sample chamber consisted of a 130  $\mu$ m diameter hole drilled in a T301 gasket, preindented to a thickness of 30  $\mu$ m. A 16:3:1 methanol: ethanol:water solution was used as the pressure-transmitting

\* Corresponding author. E-mail: jiangz@zju.edu.cn. Phone: +86 571 8795 2107. Fax: +86 571 8795 1528.

<sup>†</sup> International Center for New-Structured Materials and Department of Materials Science and Engineering, Zhejiang University.

<sup>‡</sup> Department of Chemistry, Zhejiang University.

<sup>§</sup> Department of Materials, University of Ulm.

<sup>||</sup> HASYLAB am DESY.

<sup>⊥</sup> Technical University of Denmark.

<sup>#</sup> Electron Microscopy Group of Materials Science, University of Ulm.

<sup>∇</sup> Department of Solid State Physics, University of Ulm.

<sup>○</sup> High Energy Accelerator Organization.

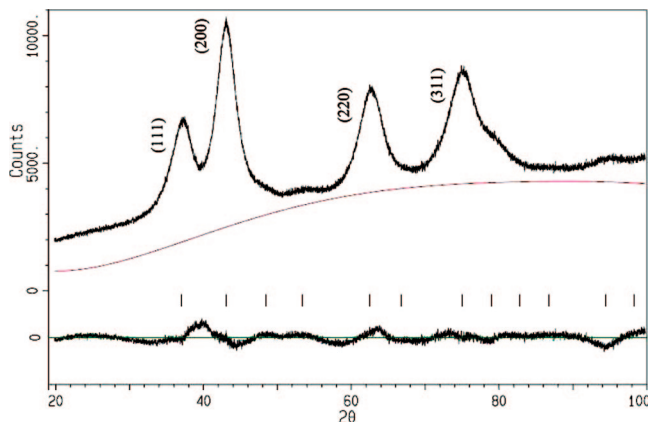


**Figure 1.** Observed and difference X-ray powder diffraction profiles for ZnO<sub>2</sub> nanoparticles prepared by the chemical method at 300 K using a Co K<sub>α</sub> radiation.

medium. The pressure was determined from the wavelength shift of the ruby line using the nonlinear pressure scale of Mao et al.<sup>12</sup> Angle-dispersive X-ray diffraction experiments were carried out using an imaging plate detector at beamline BL-13A, KEK Synchrotron Radiation Facility in Japan, at ambient temperature. The monochromatized X-ray ( $\lambda = 0.4263(2)$  Å) was collimated  $50 \times 50$  μm and irradiated to the center of the sample. Thermogravimetry (TG) measurement of ZnO<sub>2</sub> nanoparticles was performed at a heating rate of 10 °C/min. Relative optical absorption for ZnO<sub>2</sub> nanoparticles was carried out by using a Fluorolog 3. The dc magnetization measurements were performed with a SQUID magnetometer (MPMSXL, Quantum Design) at 5, 10, and 60 K.

**Simulation.** The first-principles calculations presented in this work were performed within the density functional theory, using Vienna ab initio simulation package (VASP) that implements the projector augmented wave (PAW) method.<sup>13,14</sup> The local density approximation (LDA)<sup>15</sup> was used for the exchange-correlation potentials. The calculations were performed using an energy cutoff of 500 eV for the plane wave basis set. Integrations in the Brillouin zone were performed using k points generated with  $12 \times 12 \times 12$ . In the geometrical optimization, all forces on atoms were converged to less than 0.001 eV/Å.

## Results and Discussion

The XRD diffraction pattern was collected in the  $2\theta$  range 20–100° in a step of 0.02° degree and counting time 2 s per step. Figure 1 shows the XRD pattern of ZnO<sub>2</sub> nanoparticles. Rietveld refinement reveals that although Bragg peaks are broad, the whole XRD pattern can be well fitted using a single phase, i.e., a cubic structure with space group of Pa $\bar{3}$  and lattice parameter of 4.874(1) Å, which is in good agreement with 4.871(6) Å reported.<sup>16</sup> Zn and O ions are located at (0, 0, 0) and (0.413, 0.413, 0.413), respectively. This is also in good agreement with Zn (0, 0, 0) and O (0.412, 0.412, 0.412) obtained from first-principles calculations. The average particle size is found to be 3.1(3) nm. Figure 2 shows the HRTEM image of ZnO<sub>2</sub> nanoparticles with lattice spacing of about 0.28 nm for the (111) plane in the cubic ZnO<sub>2</sub>. The composition ratio of Zn to O in the sample was detected to be 1:1.9 by EELS.

Figure 3 shows TG curve and its derivative for ZnO<sub>2</sub> nanoparticles. The weight drops by 25% when temperature increases from ambient temperature to 120 °C. It remains almost constant up to 230 °C and then drops from 70% to 55% in the temperature range from 230 to 400 °C. The first weight drop

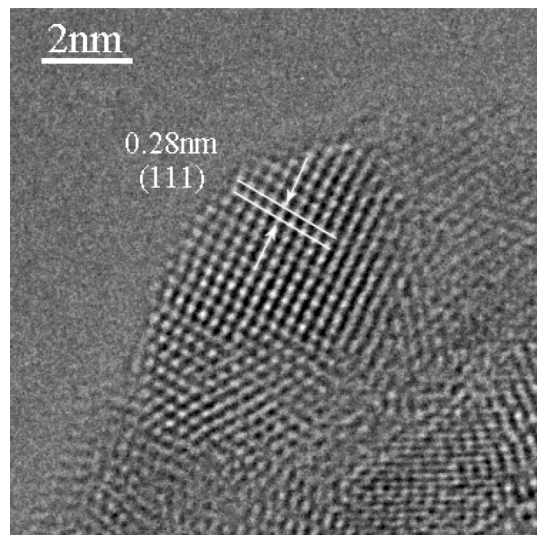


**Figure 2.** HRTEM image of ZnO<sub>2</sub> nanoparticles prepared by the chemical method, confirming a cubic structure with lattice fringe 2.8 Å of (111) plane.

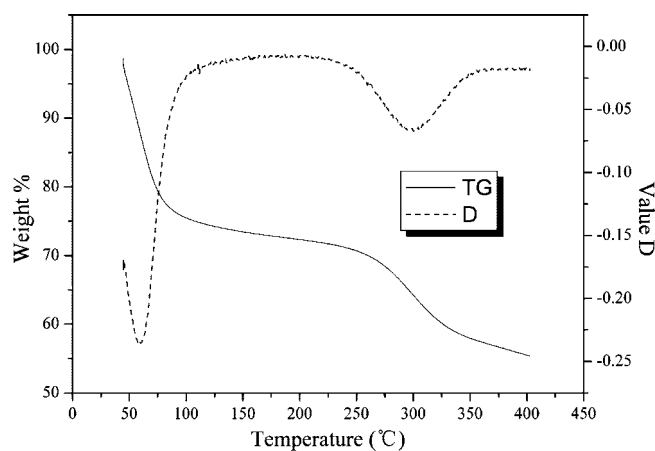


**Figure 3.** TG curve and its derivative for ZnO<sub>2</sub> nanoparticles at a heating rate of 10 K/min.

may be caused by evaporation of water for the as-prepared ZnO<sub>2</sub> nanoparticles by the chemical method. The second drop could be due to the decomposition of ZnO<sub>2</sub> into ZnO and oxygen ( $2\text{ZnO}_2 = 2\text{ZnO} + \text{O}_2$ ).<sup>17</sup> To further study temperature-induced weight loss of as-prepared ZnO<sub>2</sub> nanoparticles, in situ high temperature XRD measurements were performed. XRD patterns of ZnO<sub>2</sub> nanoparticles in Figure 4 exhibit rather broad peaks, indicating its nanocrystalline nature with the cubic structure at low temperatures below 230 °C. No phase transition occurs in the temperature range of 50–120 °C for the first weight loss. After reaching a temperature of 230 °C, a hexagonal ZnO phase was observed, is stable up to 800 °C, and remains after cooling to ambient temperature. These results confirm that the second weight loss at around 230 °C in Figure 3 is indeed due to the decomposition of the ZnO<sub>2</sub> cubic phase into the hexagonal ZnO phase.

To further investigate the stability of ZnO<sub>2</sub> nanoparticles at high pressure, the high pressure angle-dispersive XRD was performed up to 36 GPa at ambient temperature. No new peaks were detected, and none of the existing peaks for the cubic phase disappear. Thus, it can be confirmed that ZnO<sub>2</sub> nanoparticles with an average particle size of 3.1 nm still remain a cubic structure up to at least 36 GPa. Some selected XRD patterns at various pressures are shown in Figure 5. Because of the nonhydrostatic

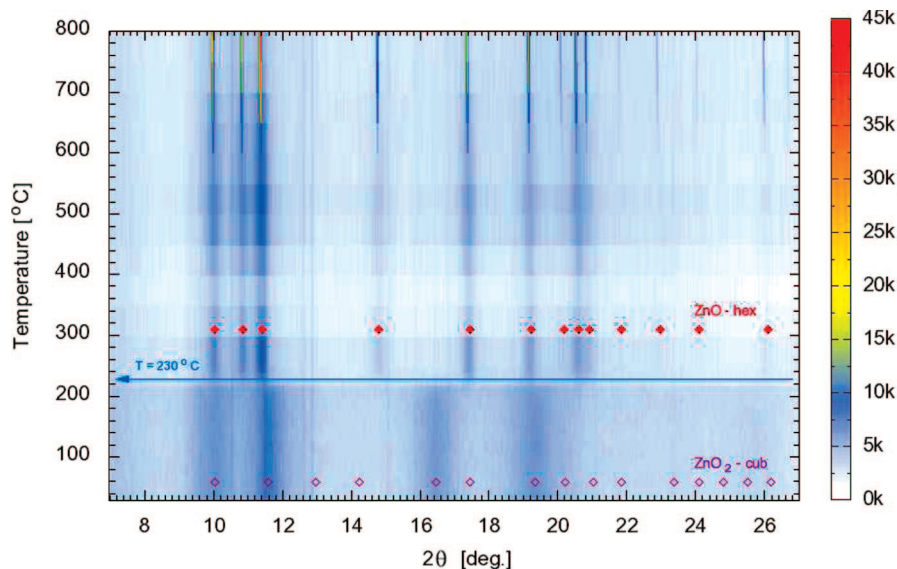


**Figure 4.** In situ high temperature XRD patterns recorded for ZnO<sub>2</sub> nanoparticles powder using a wavelength 0.49334(5) Å.

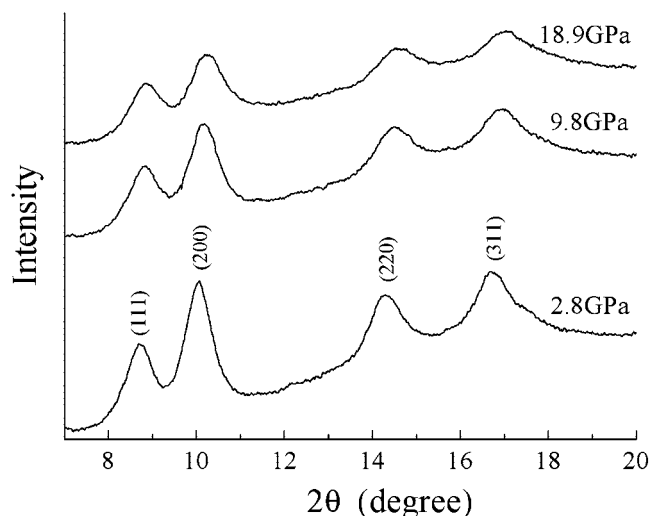


**Figure 5.** Three in situ high pressure XRD patterns recorded for ZnO<sub>2</sub> nanoparticles at 2.8, 9.8, and 18.9 GPa using a wavelength 0.4263(2) Å.

effect of the pressure medium at high pressures, lattice parameters only at low pressure range below 14 GPa were used to estimate the compressibility of ZnO<sub>2</sub> nanoparticles, as shown in Figure 6, in which both results obtained from experiments and first-principles calculations are plotted. The compression data can be used to determine the bulk modulus ( $B_0$ ) at zero pressure of cubic ZnO<sub>2</sub> nanoparticles.  $B_0$  is defined as the reciprocal of the volume compressibility at zero pressure. The P–V data were fitted using a Birch–Murnaghan equation of state:

$$P = 1.5B_0[(V/V_0)^{-7/3} - (V/V_0)^{-5/3}][1 - 0.75(B_0' - 4)[1 - (V/V_0)^{-2/3}] \quad (1)$$

The total energy vs different volumes obtained from first-principles calculations were fitted to the Murnaghan equation of state as below:

$$E(V) = E_0 - \frac{B_0 V_0}{B_0' - 1} + \frac{B_0 V}{B_0'} \left[ \frac{(V_0/V)^{B_0'}}{B_0' - 1} + 1 \right] \quad (2)$$

where  $B_0'$  is the pressure derivative at zero pressure and  $E_0$  is the ground-state total energy. The results obtained from calcula-

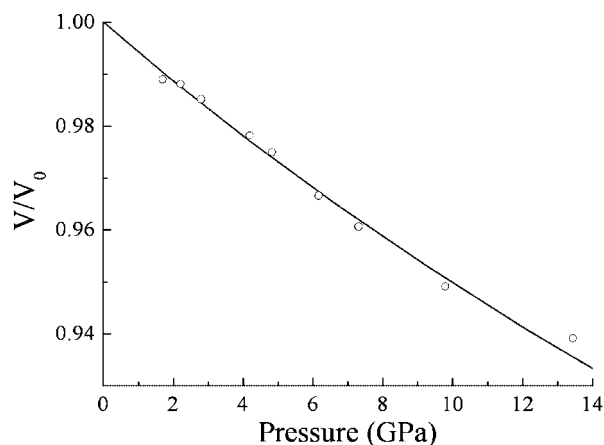


**Figure 6.** Pressure-volume relationship for ZnO<sub>2</sub> nanoparticles together with results obtained from first-principles calculations. Open circles refer to the experimental data, and the solid line refers to the calculation data.

**TABLE 1: Volume per Unit Cell  $V_0$  (Å<sup>3</sup>), Lattice Parameter  $a_0$  (Å), Bulk Modulus  $B_0$  (GPa), Pressure Derivative of Bulk Modulus at Zero Pressure  $B_0'$ , and Energy Gap  $E_g$  (eV) of ZnO<sub>2</sub> at Zero Pressure.**

	$V_0$	$a_0$	$B_0$	$B_0'$	$E_g$
high pressure expt	117.3(1)	4.895(5)	153(4)	10.3(5)	
high pressure expt			184(7)	4(fix)	
high pressure expt			174(5)	4.71(fix)	
Rietveld refinement		4.874(1)			
remission spectrum					4.5(5)
first-principles calculation	111.8	4.817	171	4.71	3.3–4.6

tion and experiments match each other well in Figure 6. All parameters are listed in Table 1. The results obtained from first principles calculations are  $B_0 = 171$  GPa,  $B_0' = 4.71$ , and  $V_0 = 111.75$  Å<sup>3</sup> for ZnO<sub>2</sub>. In order to compare results obtained from calculations with results obtained from experimental data, experimental data were fitted in three ways: (1)  $B_0'$  is a free fitting parameter, (2)  $B_0'$  is constrained to 4, which is usually assumed for solid materials, and (3)  $B_0'$  is constrained to 4.71, which is the value obtained from first-principles calculations. It is obtained that  $B_0 = 153(4)$  GPa,  $B_0' = 10.3(5)$  when  $B_0'$  is unconstrained,  $B_0 = 184(7)$  GPa when  $B_0'$  is constrained to 4,

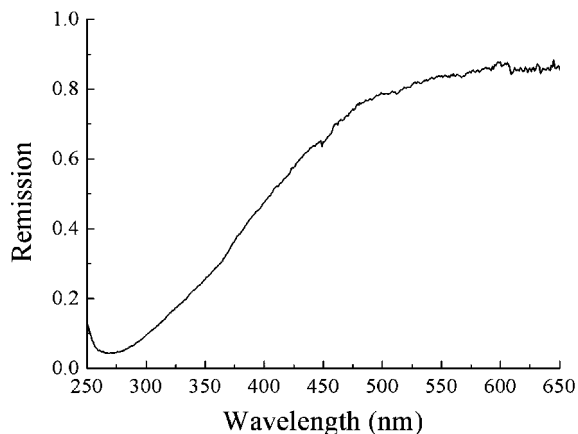


**Figure 7.** Optical remission spectrum for ZnO<sub>2</sub> nanoparticles at ambient temperature.

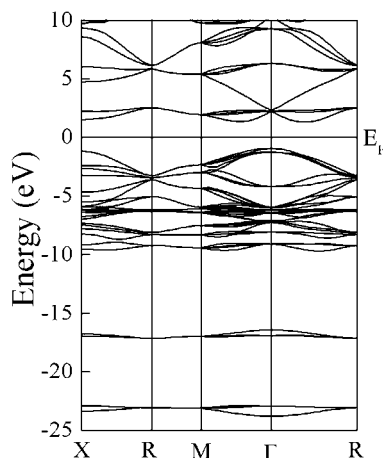


**Figure 8.** Calculated band structure for ZnO<sub>2</sub> at 0 K.

and  $B_0 = 174(5)$  GPa when  $B_0'$  is constrained to 4.71. When  $B_0' = 4.71$ ,  $B_0$  is almost the same for both calculation and experiment. It is known that the higher the  $B_0'$ , the lower the  $B_0$ . Thus, we believe that our ZnO<sub>2</sub> nanoparticle has a bulk modulus of about 174(5) GPa. The lattice parameter at zero pressure is  $a_0 = 4.817$  Å from calculations and  $a_0 = 4.895(5)$  Å from high-pressure experimental data. For  $a_0$ , the experimental value of 4.895(5) Å is closed to the Rietveld refinement result of 4.874(1) Å which was obtained from the normal XRD using a Co source at ambient conditions. The difference between the lattice parameter obtained from calculations and experiments might be caused by the following: (1) the lattice parameter is usually underestimated by using LDA, (2) the temperature effect on the lattice parameter because the value deduced from experiments at room temperature and the value deduced from calculation is at 0 K, and (3) there might be difference between nanometer-sized (experiments) and bulk (calculations) ZnO<sub>2</sub>.

A remission spectrum of ZnO<sub>2</sub> nanoparticles at room temperature is shown in Figure 7. The band gap value calculated from remission edge is about 4.5(5) eV, which is also confirmed by PL spectrum measurements and is between the value of 3.71 eV for annealed ZnO<sub>2</sub> film on quartz and the value of 5.7 eV for the as-grown ZnO<sub>2</sub> film on quartz.<sup>18</sup> To have a clear electronic structure of ZnO<sub>2</sub>, band structure and partial density of states (PDOS) are calculated by first-principles simulation in Figures 8 and 9, respectively. It is found that there is a strong hybridization between Zn-d and O-p states. ZnO<sub>2</sub> is an indirect semiconductor with the top of the valence band located at  $\Gamma$  and the bottom of the conduction band located between  $\Gamma$  and

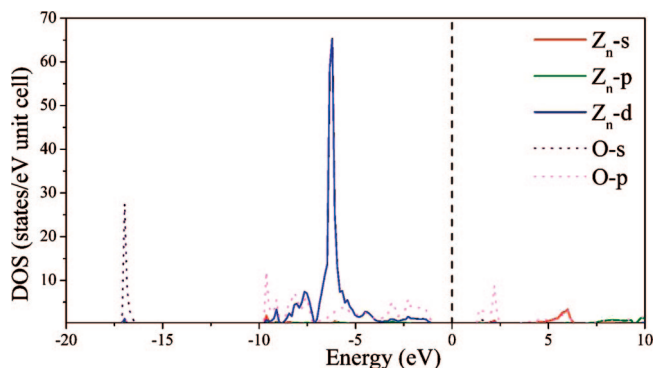


**Figure 9.** Calculated density of states for ZnO<sub>2</sub> at 0 K.

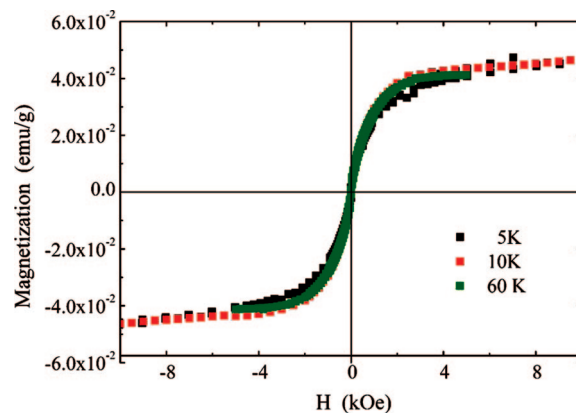


**Figure 10.** Magnetization as a function of magnetic field for ZnO<sub>2</sub> nanoparticles at 5, 10, and 60 K.

R. The indirect energy gap is 2.3 eV. It is well-known that the band gap is generally underestimated by about 50–100% using density functional theory.<sup>19</sup> Hence, the real value of the energy gap for ZnO<sub>2</sub> could be in the range of 3.3–4.6 eV, in agreement with the value calculated from remission spectrum. Though the calculated energy gap is a little lower, the quantum effect of small crystallite size, which most likely enhances the energy gap,<sup>20</sup> was not taken into account in the present simulation. Figure 10 shows magnetization as a function of magnetic field for ZnO<sub>2</sub> nanoparticles at 5, 10, and 60 K. It is found that within experimental uncertainty no magnetic hystereses were detected for ZnO<sub>2</sub> nanoparticles down to 5 K, indicating a paramagnetic state for the sample.

## Conclusions

In summary, ZnO<sub>2</sub> nanoparticles with an average particle size of 3.1(3) nm have been synthesized by a chemical method. It has a cubic structure with space group of Pa $\bar{3}$  and lattice parameter of 4.874(1) Å. Zn and O ions are located at (000) and (0.413, 0.413, 0.413), respectively, and a composition of the nanoparticles is Zn:O = 1:1.9. This cubic ZnO<sub>2</sub> nanoparticle is stable up to 230 °C at ambient pressure and up to 36 GPa at ambient temperature. It decomposes into ZnO at temperatures above 230 °C. The cubic ZnO<sub>2</sub> phase has a bulk modulus of  $B_0 = 174(5)$  GPa and a pressure derivative  $B_0' = 4.71$  at zero pressure, compared to  $B_0 = 171$  GPa when  $B_0' = 4.71$  from first principles calculations. This nanocrystalline ZnO<sub>2</sub> material is an indirect semiconductor with an energy gap of about 4.5(5) eV and is paramagnetic down to 5 K.

**Acknowledgment.** The authors thank HASYLAB in Hamburg, Germany, KEK SPring8 in Japan, BSRF in Beijing, and

NSRL in Hefei, P. R. China, for use of the synchrotron radiation facilities. Financial support from the National Natural Science Foundation of China (grant nos. 50425102, 50601021, 50701038, 60776014, 60876002, and 10804096), Zhejiang University-Helmholtz cooperation fund, the Ministry of Education of China (Program for Changjiang Scholars and the Research Fund for the Doctoral Program of Higher Education), the Department of Science and Technology of Zhejiang province and Zhejiang University is gratefully acknowledged.

### References and Notes

- (1) Gleiter, H. *Acta Mater.* **2000**, *48*, 1–29.
- (2) Philip, M. *Rep. Prog. Phys.* **2001**, *64*, 297–381.
- (3) Ibarra, L.; Alzoriz, M. *Polym. Int.* **1996**, *48*, 550–586.
- (4) Ibarra, L.; Alzoriz, M. *J. Appl. Polym. Sci.* **2002**, *84*, 605–615.
- (5) Ibarra, L.; Alzoriz, M. *Polymer* **2002**, *43*, 1649–1655.
- (6) Ohno, S.; Aburatani, N.; Ueda, N. DE Patent 2,914,058, 1980.
- (7) Ohno, S.; Aburatani, N.; Ueda, N. DE Patent 4,247,412, 1981.
- (8) Hagel, R.; Redecker, K. US Patent 4,363,679, 1982.
- (9) Uekawa, N.; Kajiwara, J.; Mochizuki, N.; Kakegawa, K.; Sasaki, Y. *Chem. Lett.* **2001**, *7*, 606–607.
- (10) Uekawa, N.; Mochizuki, N.; Kajiwara, J.; Mori, F.; Wu, Y. J.; Kakegawa, K. *Phys. Chem. Chem. Phys.* **2003**, *5*, 929–934.
- (11) Jiang, J. Z.; Lin, R.; Nielsen, K.; Mørup, S.; Rickerby, D. G.; Clasen, R. *Phys. Rev. B* **1997**, *55*, 14830–14835.
- (12) Mao, H. K.; Bell, P. M.; Shaner, J. W.; Steinberg, D. J. *J. Appl. Phys.* **1978**, *49*, 3276.
- (13) Kresse, G.; Furthmüller, J. *Phys. Rev. B* **1996**, *54*, 11169.
- (14) Kresse, G.; Joubert, D. *Phys. Rev. B* **1999**, *59*, 1758.
- (15) Ceperley, D. M.; Alder, B. J. *Phys. Rev. Lett.* **1980**, *45*, 566.
- (16) Vannerberg, N. G. *Ark. Kemi* **1959**, *14*, 119.
- (17) Sun, M.; Hao, W. C.; Wang, C. Z.; Wang, T. M. *Chem. Phys. Lett.* **2007**, *443*, 342–346.
- (18) Lindross, S.; Leskela, M. *Int. J. Inorg. Mater.* **2000**, *2*, 197.
- (19) Majewski, J. A.; Birner, S.; Trellakis, A.; Sabathil, M.; Vogl, P. *Phys. Status Solidi C* **2004**, *1*, 2003.
- (20) Brus, L. E. *J. Chem. Phys.* **1984**, *80*, 4403.

JP808714V